Optics and Laser Technology 111 (2019) 271–283

Contents lists available at ScienceDirect

Optics and Laser Technology

journal homepage: www.elsevier.com/locate/optlastec

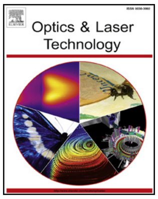

Full length article

Comparative study on microstructure and corrosion performance of 316 stainless steel prepared by laser melting deposition with ring-shaped beam and Gaussian beam

Jianbo Lei[a,b,*], Jichang Xie[a,*], Shengfeng Zhou[a], Heyu Song[a], Xinling Song[a], Xiaoyu Zhou[b,c]

[a] *Laser Technology Institute, Tianjin Polytechnic University, Tianjin 300387, China*
[b] *Tianjin Engineering Research Center of Near-Net-Shape Forming Technology for Metallic Materials, Tianjin 300384, China*
[c] *School of Materials Science and Engineering, Tianjin University of Technology, Tianjin 300384,China*

HIGHLIGHTS

- Ring-shaped laser beam was employed and optimized for 316ss cladding.
- Finer grains were achieved by using ring-shaped laser beam compared with those obtained from the Gaussian beam.
- Enhanced electrochemical performance was achieved using ring-shaped beam cladding.

ARTICLE INFO

Keywords:
316 stainless steel
Laser melting deposition
Ring-shaped laser beam
Microstructure
Electrochemical corrosion

ABSTRACT

Compared with the Gaussian laser beam, the ring-shaped laser beam has the advantages of uniform energy distribution and small temperature gradient. During the laser melting deposition, the ring-shaped beam can produce smaller residual stress in the workpiece, meanwhile avoids excessive sintering and dilution, reduces the heat accumulation, refines the grain size and improves the surface quality of the coating. In this study, hollow-laser beam melting deposition with internal powder feeding (HLB-MD-IPF) and regular Gaussian beam were compared to explore the effect of laser beam shape on the quality of coatings. The microhardness and electrochemical corrosion performance of the 316 stainless steel coatings prepared by different processing parameters were studied. The intrinsic mechanism of the performance difference was analyzed through microstructure and element distribution, and compared with the traditional Gaussian beam. In HLB-MD-IPF, the maximum microhardness was obtained with laser scanning speed of 12 mm/s, powder delivery rate of 1.6 rpm and laser power of 700 W, respectively. The average microhardness of the coatings prepared by different processes was between 270 and 310HV$_{0.2}$. It was found that the microhardness of the coating decreased with the coarsening of the microstructure. Our results showed that with the same processing parameters, the microstructure prepared by the HLB-MD-IPF was obviously finer than those obtained from the Gaussian beam.

1. Introduction

316 stainless steel has been widely used in many fields due to its good ductility, high strength [1,2] and good corrosion resistance [3], such as petrochemical [4,5], chemical [6], biological materials [7–9], and nuclear engineering [10,11], etc. Traditional stainless steel workpieces are mainly made by casting [12], forging [13] or squeeze casting [14]. However, these technologies can not directly produce complex workpieces, instead post-treatment or welding are required to produce such workable parts, resulting in waste of energy, materials and time [15]. Laser additive manufacturing (AM) technology has attracted wide attention, especially in automotive, aerospace and medical fields [16], due to its flexibility to directly prepare workpieces with special requirements, such as complex shape and functionally gradient properties [17].

A lot of research has been conducted on the 316 stainless steel by laser melting deposition (LMD), but most of these studies use Gaussian beam (energy is Gaussian distribution), resulting in the absorption of energy at the center of the molten pool is higher than the periphery during the laser cladding process. As a result, during the cooling, the

---

* Corresponding authors.
E-mail addresses: ljbtj@163.com (J. Lei), xjctjpu@163.com (J. Xie).

https://doi.org/10.1016/j.optlastec.2018.09.057
Received 24 May 2018; Received in revised form 22 September 2018; Accepted 30 September 2018

periphery will solidify earlier than the center of the molten pool, which will cause the nonuniformity of the cladding structure. It is known that during solidification, the change of volume will lead to the residual stress. With the increase of cladding thickness, excessive residual stress tends to cause warping and cracking of the cladding layer or the workpiece [18,19]. 316 stainless steel is difficult to conduct heat treatment because of its low carbon content. Therefore, how to reduce its internal residual stress has become a serious problem in practical application.

In order to solve this problem, a ring-shaped laser beam is proposed, and used in the quenching experiment by Li et al. [20], where the edge energy is higher than the central energy. The temperature distribution of the ring-shaped beam has also been simulated in the previous study [21], showing reduced central temperature of the molten pool and improved uniformity of energy distribution in the laser scanned area [22]. Due to the decrease of the central temperature of the molten pool, the corresponding melting depth will also be reduced, while maintaining good metallurgical bonding. On the other hand, the dilution rate of the cladding layer or the thermal influence on the previous layer will also be reduced, thereby avoiding excessive sintering and making the microstructure formed by cladding layer more compact. Besides, it also avoids over-sintering and forms finer microstructure of the coating.

In this study, the hollow-laser beam with internal powder feeding (HLB-IPF) is applied [23], where the gas and powder feeding tubes are placed inside the ring-shaped laser beam. The powders are heated and melted when they are exposed to the converged laser beam during its vertical falling. This strategy realizes coaxial powder feeding, which not only improves the utilization ratio of powder and cladding efficiency at the same time, but also makes the cladding surface smoother. Here, the microstructures of the specimens prepared by the ring-shaped laser beam and by the traditional Gaussian beam are compared, and correlated to the microhardness and corrosion properties.

2. Experimental materials and procedures

2.1. Experimental materials

The substrate material used in this work was 304 stainless steel (304ss) with the dimension of 100 mm × 60 mm × 5 mm. The chemical composition of 304ss was composed of C0–0.08, Si0–1.0, Mn0–2.0, Ni8.0–11.0, Cr18.0–20.0, and Fe Bal. (wt%).The cladding metal was 316 stainless steel (316ss) powder prepared by atomization method, which was composed of C0–0.08, Si0–1.0, Mn0–2.0, Ni10.0–14.0, Cr16.0–18.0, Mo2.0–3.0, and Fe Bal. (wt%). The morphology of the 316ss powders were shown in Fig. 1, with particle size ranging from 30 to 70 μm. The main components of 316ss and 304ss are basically the same, however, Mo is added to the 316ss. Thus, the interface of the cladding layer and the substrate can be analyzed through the diffusion of Mo element.

Fig. 1. Morphology of the 316ss powders.

2.2. Experimental procedures

Single-track and multiple-track of 316ss cladding were prepared using different laser beams in this study.

The HLB-IPF head (as shown in Fig. 2a) with series number of JGRF-102-2 has a ring-shaped beam [23], and its energy distribution is shown in Fig. 2c. Nitrogen was used for powder feeding to prevent the powder from oxidation during the melting process and to reduce the scattering and absorption of the laser energy by the plasma due to the ionizing effect. IPG ytterbium doped fiber laser with model of YLS-2000-TR 2 kW and wavelength of 1064 nm was used. The outer and inner diameter of the ring-shaped beam is 1.8 and 0.8 mm respectively. KUKA robot KR60-3F with programming language of KRL, an external rotation platform and GTV PF2/2 powder feeding system were employed. Based on the above setup, the corresponding processing parameters are as listed in Table 1.

Unlike the HLB-MD-IPF, in coaxial powder feeding head used by traditional method [24], the dispersed metal powder is converged through high pressure nitrogen and sent to the Gaussian beam perpendicular to the substrate. For typical CO_2 laser with model of GS-TFL-6000 6 kW and wavelength of 10.6 μm, given a Gaussian beam size of 2.5 mm, its distribution of energy density is like the one shown in Fig. 2b.

Although the area of ring-shaped is slightly smaller, the energy input of ring-shaped beam was substantially the same as the Gaussian beam. This experiment aims to investigate the cladding effect under the same energy input, and since the coaxial powder feeding heads are specially designed, unifying their spot size will have a negative impact on the actual cladding effect, so the experimental comparison of the optimal spot conditions was adopted.

The prepared cladding layer was inlaid by the epoxy resin powder after cutting down by the electro-spark cutting machine. Then the specimen was mechanically grounded and polished. Microhardness distribution of the coating was measured by a HV-1000 Vickers digital microhardness tester with a load of 1.96 N and a dwell time of 10 s. The microhardness test started from the top of the coating along the center line of the cross section, through the heat affected zone (HAZ) until the substrate was carried out after the Marble solution corrosion, as indicated in Fig. 3.

The microstructure and element distribution of coatings were analyzed by ZEISS Sigma 300 field emission scanning electron microscopy (SEM) equipped with X-ray energy-dispersive spectrometer (EDS) at an accelerating voltage of 20 kV. A D/MAX-2500 X-ray diffraction (XRD) instrument was used to analyze the phases of coatings (Cu target, 40 kV, 140 mA).

In order to investigate the influence of different processing parameters and the shape of laser beam on the corrosion resistance of 316ss coating, the electrochemical resistance was measured by the CHI604e electrochemical analyzer (Shanghai, China), due to the wide application of 316 stainless steel in the marine industry, a solution concentration close to sea water (3.5% NaCl solution) was employed for the corrosion resistance test. A three-electrode cell was used for the measurements, where a saturated calomel electrode (SCE) was used as the reference electrode and a platinum (Pt) foil was used as the counterpart. The specimens with an exposed area of about 1 cm^2 were used as the working electrode. All specimens were immersed in the test electrolyte at room temperature for 1 h to stabilize the open circuit potential (OCP). The potentiodynamic polarization scanning was varied from -0.9 to $+0.9$ V, and the sweeping rate was 5 mV/s. The corresponding corrosion current density (icorr) and corrosion potential (Ecorr) were determined using the Tafel extrapolation method. Electrochemical impedance spectroscopy (EIS) tests were performed at the OCP with an AC amplitude of 10 mV in the frequency range between 10^4 and 10^{-2} Hz.